Indian Journal of Chemical Technology
Vol. 33, September 2026, pp. 698-710
DOI: 10.56042/ijct.v33i5.27935

Ficus carica leaves extract as a corrosion protector for oil-well steel API P110 in sulfuric acid solution, synergistic effect

Kamilia Chahrazed Ksir[1,2]*, Mina Boulkroune[1,2] & Lamis Touati[1,2]

[1] Environmental and Structural Molecular Chemistry Research unit (UR-CHEMS) /University Mentouri Brothers, Constantine, 25000, Algeria

[2] Department of Chemistry, Faculty of Exact Sciences/University Mentouri Brothers, Constantine, 25000, Algeria

*E-mail: kamilia-chahrazed.ksir@doc.umc.edu.dz

Received 25 January 2026; accepted 6 August 2026

The corrosion prevention of steel API 5CT (P110) using an extract from *Ficus carica Leaves* (FCL) in H_2SO_4 solution (0.5M) was examined by electrochemical impedance spectroscopy, weight loss, and potentiodynamic polarization methods at 298 K. The findings indicate that as the temperature and concentration of the extract increases, its inhibitory efficiency also does. The Temkin adsorption isotherm is the most effective way to describe the inhibitor adsorption properties. The inhibitor exothermic and spontaneous adsorption occurs on steel surface with both chemical and physical adsorption processes. Synergistic combinations with halides (Br^-, I^-) improve the adsorption of the inhibitor reaching inhibition efficiency values superior than 99% at low concentrations. The composition of the extract was analyzed by FT-IR and the surface state was carried out by SEM. According to the study, it is possible to successfully prevent an oil-well steel API P110 from corrosion in acidic environment (0.5 M H_2SO_4) using an ethanol extract of FCL achieving high efficiencies at low costs without damaging the environment.

Keywords: Acidic environment, Corrosion inhibitor, Electrochemical, surface analysis, *Ficus carica* leaves, Steel, Synergy

Introduction

Metals, particularly steels, play a pivotal role in modern industry owing to their excellent mechanical properties, cost-effectiveness, and versatility. They are extensively employed in critical applications, including transportation systems, construction, power generation facilities, petrochemical plants, and oil and gas production equipment. Despite these advantages, steel structures are highly susceptible to corrosion because of their iron-rich composition, especially when exposed to aggressive acidic environments. Such media are commonly encountered during industrial operations, including acid pickling, oil-well acidizing, industrial cleaning, and chemical processing, where severe corrosion may compromise equipment integrity, operational safety, and economic performance[1,2].

Among the steels used in the petroleum industry, API P110 and API L80 are widely employed as casing and tubing materials. API L80 steel is generally preferred in sour environments because of its higher resistance to sulfide stress cracking, whereas API P110 steel is extensively utilized in deep and high-pressure wells owing to its superior mechanical strength. Nevertheless, its greater susceptibility to acid corrosion remains a major challenge during well stimulation and acidizing treatments[3-5].

Corrosion is an unavoidable electrochemical process that results in substantial economic losses, safety concerns, and environmental impacts worldwide. Among the various corrosion mitigation strategies, the use of corrosion inhibitors remains one of the most practical, efficient, and economical approaches. Corrosion inhibitors reduce the corrosion rate by adsorbing onto the metal surface and forming a protective barrier that limits the interaction between the metallic substrate and the aggressive medium.

In recent years, increasing environmental awareness and stricter regulations concerning hazardous chemicals have stimulated considerable interest in developing sustainable and environmentally benign corrosion inhibitors. Plant extracts have emerged as promising green alternatives because they are renewable, biodegradable, readily available, and rich in naturally occurring phytochemicals capable of interacting strongly with metallic surfaces, thereby enhancing corrosion protection. Consequently, numerous plant extracts have demonstrated remarkable inhibition efficiencies for steels in acidic media[6,9].

Ficus carica, a member of the Moraceae family, is recognized as an abundant source of bioactive compounds with strong antioxidant activity, particularly flavonoids and phenolic acids. Owing to these properties, extracts from its leaves have attracted increasing attention as environmentally friendly corrosion inhibitors. Previous studies have demonstrated the corrosion inhibition performance of *Ficus carica* leaves (FCL) extracts for various steels in different acidic environments using various extraction solvents[10-13]. However, studies addressing the protection of API P110 steel remain scarce, despite its widespread application in deep and high-pressure oil wells. Furthermore, the synergistic effect of halide ions has been reported for several organic and plant-derived inhibitors[14], these investigations have mainly focused on iodide ions, while comparative studies involving both iodide and bromide ions remain also scarce, especially FCL extract for API P110 steel.

Therefore, the novelty of the present study lies in investigating the corrosion inhibition performance of FCL ethanol extract for high-strength API P110 steel in 0.5 M H_2SO_4, together with the synergistic action of iodide (I^-) and bromide (Br^-) ions. In addition to evaluating the inhibition efficiency of the extract, special attention is given to comparing the influence of the two halide ions on the adsorption behaviour, and surface protection of API P110 steel. The inhibition mechanism is elucidated through a combination of gravimetric measurements, electrochemical techniques, surface characterization (SEM, FTIR and UV–visible analyses), and adsorption studies, while the effects of inhibitor concentration, temperature, and storage time of the inhibitor solution are also examined. By integrating these complementary approaches, this work provides a deeper understanding of the interaction between FCL extract, halide ions, and high-strength steel, and offers valuable insights for the development of environmentally friendly corrosion inhibitors for oil-field applications.

Experimental Section

Materials

Metal preparation

In our analysis, we used (API 5CT (P110)) steel samples composed of 0.31 % of carbon (C), 0.58 % of manganese (Mn), 0.33 % of silicon (Si), 0.0025 % of chromium (Cr), 0.0018 % of phosphorus (P), 0.98 % of molybdenum (Mo), 0.61 % of aluminum (Al), 0.022 % of niobium(Nb), 0.038 % of copper (Cu) and the rest is the iron (Fe). For the electrochemical testing, a steel working electrode with an exposed area of 0.5024 cm^2 was utilized, whereas samples with 5.76 cm^2 surface were used for the gravimetric approach. A series of emery papers (220, 400, 600, 800, 1200, 2000) were used to mechanically abrade the sample before each test. To ensure that the tests can be replicated, the sample was properly cleaned using distilled water, degreased using acetone, and allowed to air dry.

Acidic environment preparation

To prepare the aggressive environment, distilled water was used to dilute sulfuric acid (M=98.08 g/mol, P=95-97%, d=1.84) to a (0.5M) solution.

Extract Preparation

Ficus carica leaves were gathered from the Constantine (Algeria), air-dried, and then ground into fine grains using an electric blender.

10 g of the dried and crushed FCL were macerated with 50 mL of ethanol at room temperature (297-298K) then filtered after 24 h, to prepare the alcoholic extract.

Methods

Electrochemical techniques

Tafel polarisation and impedance curves were recorded using a potentiostat/galvanostat ZRA "GAMRY-Reference 3000" that was set up using the Gamry Framework Software. A working (steel), auxiliary (Pt), and reference (SCE) electrodes were utilized.

After 30 min of steady state, the Tafel curves were recorded, at a scan rate of 1 mV/s, between -800 and -200 mV. The following formula was used to calculate the inhibitory efficiency[15]:

$$IE\ (\%) = \frac{I_{0\ corr} - I_{corr}}{I_{0\ corr}} \times 100 \quad \ldots (1)$$

Where, $I_{o\ corr}$ and I_{corr} are the corrosion current densities in absence and presence of FCL extract, respectively.

With a peak-to-peak capacitance of 10 mV, the Nyquist format used to display the impedance diagram curves were captured between 100 kHz and 0.1 Hz. The inhibition efficiency can be determined using the formula given below[15]:

$$IE\ (\%) = \frac{R_{ct} - R_{0\ ct}}{R_{ct}} \times 100 \quad \ldots (2)$$

Where, $R_{0\ ct}$ and R_{ct} are the charge transfer resistances in absence and presence of FCL extract, respectively.

Weight loss method

After preparation, the steel samples were submerged in aggressive H_2SO_4 solutions (0.5 M) with diverse concentrations of FCL extract (1000–5000 ppm) for two hours. After cleaning, a precise weight measurement was performed. The inhibition efficiency was computed using the formula given below[15]:

$$IE\ (\%) = \frac{CR_0 - CR}{CR_0} \times 100 \quad \ldots (3)$$

Where, CR_0 and CR are corrosion rates in absence and presence of FCL extract, respectively.

The corrosion rate (CR) is calculated using Eq. (4)[16]:

$$CR = \frac{m_1 - m_2}{A \times t} \quad \ldots (4)$$

Where, m_1 and m_2 are the initial and final masses of the API P110 steel specimen before and after immersion, respectively; A is the exposed surface area of the specimen (cm^2), and t is the immersion time (h).

And the surface coverage (θ) by the Eq. (5).

$$\theta = \frac{IE\ (\%)}{100} \quad \ldots (5)$$

All gravimetric and electrochemical experiments were repeated independently (2–5 replicates depending on the experiment). The reported values are presented as mean ± standard deviation, and error bars have been added where applicable.

UV-visible spectral analysis

UV-visible spectra were recorded with an Agilent Technologies Cary 60 UV spectrometer with a quartz cuvatte.

FT-IR analysis

The FT-IR spectra were recorded by ATR Senterra 6400 spectrometer.FCL liquid extract and the film formed on the steel surface after exposure to the inhibited solution spectra were recorded.

SEM analysis

The apparatus model used was MEB-FEG: Quattro S. The surface micrography was recorded for different samples of steel before and after immersion for two hours in H_2SO_4 solution (0.5 M), without and with 5000 ppm of FCL extract, and after the addition of 10^{-2} M of KBr then KI to the inhibited solution.

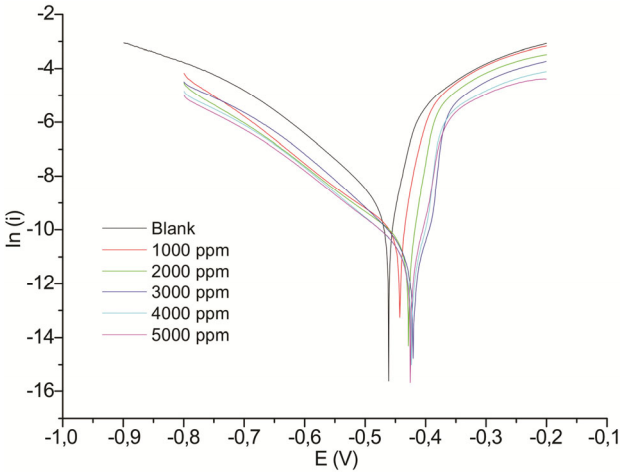

Fig. 1 — Tafel curves for API P110 steel corrosion in H_2SO_4 solution without and with different concentrations of FCL extract at 298 K

Results and Discussion

Tafel polarization

The Tafel curves of steel in 0.5 M H_2SO_4without and with the addition of various concentrations (1000–5000 ppm) of FCL extract are displayed in Fig. 1. The addition of the extract to the aggressive solution decreased both cathodic and anodic current densities. This suggests a reduction in the anodic dissolution of steel and a delay in the cathodic hydrogen evolution reaction.

Table 1 lists the corrosion current density (I_{corr}), the corrosion potential (E_{corr}), and the cathodic and anodic Tafel slopes (β_c and β_a) obtained from the extrapolation of the anodic and cathodic sections of the Tafel plots. According to the Table 1, the corrosion potential (E_{corr}) shifts toward more positive values, indicating that the steel surface becomes more noble. Since the shift in E_{corr} is less than 85 mV, FCL extract can be classified as a mixed-type corrosion inhibitor[17,18].

Fig. 1 shows that the Tafel polarization curves exhibit a similar shape, indicating that the same corrosion mechanism is maintained in both the absence and presence of the inhibitor. Except at the highest inhibitor concentration, the anodic branch exhibits a desorption phenomenon. As shown in Table 1, the addition of the extract to the 0.5 M H_2SO_4 solution had little effect on the anodic and cathodic Tafel slopes (β_a and β_c). This suggests that the inhibitor does not alter the kinetics of either the anodic metal dissolution or the cathodic hydrogen evolution reaction[19].

Table 1 — Tafel plots parameters values for API P110 steel corrosion in 0.5M H_2SO_4 solution without and with different concentrations of FCL extract at 298K and the corresponding inhibition efficiencies

C (*ppm*)	E_{corr} (*mV /SCE*)	I_{corr} ($\mu A/cm^2$)	β_c (*mV/decade*)	β_a (*mV/decade*)	*IE* (%)
Blank	- 461± 0.1101	99.50± 0.1914	114.9	38.4	/
1000	- 442.8± 0.1728	39.29± 0.1654	137.7	24.64	60.51
2000	- 428.7± 0.1647	26.58± 0.1912	135.3	26.08	73.28
3000	- 421± 0.1625	18.90± 0.1741	108.5	51.50	81
4000	- 424± 0.1524	14.70± 0.2017	116.4	33.7	85.22
5000	- 426± 0.1210	6.84± 0.1841	52.8	23	93.12

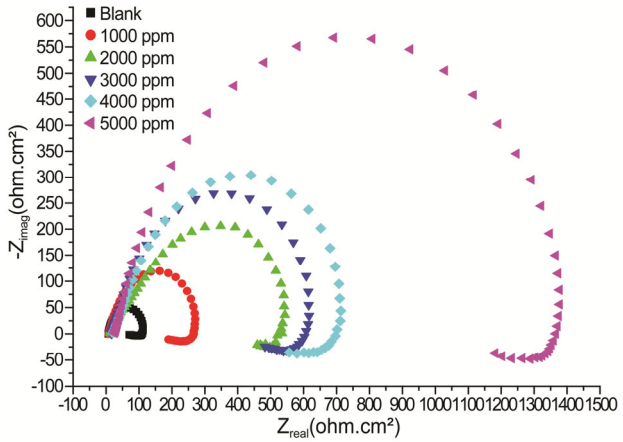

Fig. 2 — Nyquist plots for API P110 steel corrosion in H_2SO_4 solution without and with different concentrations of FCL extract at 298 K

Electrochemical impedance spectroscopy

The Nyquist curves of steel in 0.5 M H_2SO_4 before and after the addition of various concentrations (1000–5000 ppm) of FCL extract are presented in Fig. 2.

The Nyquist plots obtained at different concentrations of FCL extract exhibit a similar shape. The depressed semicircles observed at high frequencies are attributed to frequency dispersion resulting from substrate roughness and surface heterogeneity of the electrode[20]. The diameter of the capacitive semicircle increases with increasing inhibitor concentration, indicating that the corrosion process is predominantly controlled by charge transfer. At low frequencies, an inductive loop is also observed, which may be attributed to the adsorption of intermediate species on the electrode surface[11]. Notably, the shape of the impedance spectra remain unchanged with increasing inhibitor concentration, suggesting that the same inhibition mechanism operates over the investigated concentration range.

An equivalent electrical circuit was used to fit the Nyquist plots[21], as shown in Fig. 3. The impedance parameters, namely the solution resistance (R_s), charge transfer resistance (R_{ct}), constant phase

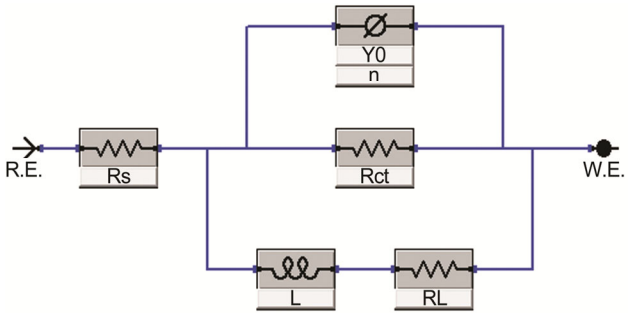

Fig. 3 — Equivalent electrical circuit used to fit the electrochemical impedance spectroscopy (EIS) data

element (CPE) parameters (where (Y_0) is the CPE constant and (n) is the CPE exponent), inductive resistance (R_L), and inductance (L), obtained from the Nyquist plots are summarized in Table 2**.** The double-layer capacitance (C_{dl}) was calculated using the following equation[11,22]:

$$C_{dl} = \frac{1}{(2\pi f_{max} R_{ct})} \quad \ldots (6)$$

Where, f_{max} is the frequency at the apex of the Nyquist plot.

The inhibition efficiency increased with increasing inhibitor concentration. The observed decrease in the C_{dl} values with increasing FCL extract concentration may be attributed to a reduction in the local dielectric constant and/or an increase in the thickness of the electrical double layer, suggesting that the FCL extract inhibits corrosion through adsorption at the metal/solution interface[23]. The decrease in C_{dl} may also be explained by the progressive replacement of water molecules adsorbed on the electrode surface by organic molecules from the FCL extract, thereby reducing the active surface area available for metal dissolution[23].

Effect of inhibitor concentration

The effect of different concentrations of FCL extract on the corrosion behaviour of steel in 0.5 M H_2SO_4 solution was investigated using the weight-loss

Table 2 — Nyquist plots parameters values of API P110 steel corrosion in 0.5M H_2SO_4 solution without and with various concentrations of FCL extract at 298 K and the corresponding inhibition efficiencies

Conc (ppm)	R_S ($\Omega.cm^2$)	R_{ct} ($\Omega.cm^2$)	Y_0 ($S^n.\Omega^{-1}.cm^{-2}$)	n	R_L ($\Omega.cm^2$)	L ($H.cm^2$)	C_{dl} ($F.cm^2$)	IE (%)
Blank	1.929	28.83± 0.1467	5.23×10^{-4}	0.8839	139.16	21.48	2.78×10^{-4}± 0.1784	-
1000	2.188	73.15± 0.1387	3.22×10^{-4}	0.8138	181.97	75.21	1.39×10^{-4}± 0.1987	60.58
2000	2.913	131.48± 0.1214	2.52×10^{-4}	0.6696	358.01	59.43	7.75×10^{-5}± 0.1957	78.07
3000	4.375	171.77± 0.1478	2.21×10^{-4}	0.7905	413.98	210.51	7.48×10^{-5} ± 0.1621	83.21
4000	5.441	240.45± 0.1399	2.73×10^{-4}	0.7519	433.27	373.58	6.67×10^{-5}± 0.1784	88.01
5000	6.757	368.96± 0.1187	1.31×10^{-4}	0.8161	2103.05	2208.05	5.43×10^{-5}± 0.1317	92.19

Table 3 — Corrosion rate (*CR*) values for API P110 steel in 0.5 M H_2SO_4 solution before and after addition of different concentrations of the FCL extract at 298 K and the corresponding surface coverage and inhibition efficiencies

	C(*ppm*)	CR($mg/h.cm^2$)	θ	*IE* (%)
Blank	-	5.556± 0.0022	-	-
FCL	1000	2.28± 0.0012	0.589	58.9
	2000	1.51± 0.0016	0.7288	72.88
	3000	1.02± 0.0013	0.8164	81.64
	4000	0.66± 0.0018	0.8806	88.06
	5000	0.44± 0.0010	0.9208	92.08

method. The corrosion rate, surface coverage, and inhibition efficiency obtained at different inhibitor concentrations are summarized in Table 3. Both the surface coverage and the inhibition efficiency increased with increasing inhibitor concentration as evident from Table 3. The FCL extract effectively covered the API P110 steel surface.

The inhibitor concentration range of 1000–5000 ppm was selected because the experimental results showed a gradual increase in inhibition efficiency with increasing extract concentration, reaching a maximum value at 5000 ppm**.** Beyond this concentration, the inhibition efficiency remained nearly constant, indicating the saturation of the steel surface by the adsorbed inhibitor molecules.

This concentration range is also relevant for field applications, as corrosion inhibitors used in oil-well acidizing operations are generally applied at ppm levels. The optimum concentration obtained in this study **(**5000 ppm, equivalent to 5 kg/m³ of acid solution**)** is therefore technically feasible for acidic oil-field environments, while providing the advantages of a plant-based and environmentally friendly inhibitor. Finally, the inhibition efficiencies determined from electrochemical impedance spectroscopy (EIS), potentiodynamic polarization, and weight-loss measurements are in good agreement, demonstrating the reliability and consistency of the obtained results.

The corrosion inhibition performance of the FCL extract obtained in the present study is also in a good agreement with previous investigations reported in the literature, although significant differences exist in the metallic substrates and testing conditions. A previous study investigated the corrosion inhibition of mild steel under practical field conditions[10], another study evaluated the performance of FCL on API L80 carbon steel in 0.5 M H_2SO_4[11]. Likewise, another investigation studied conventional carbon steel in sulfuric acid solution[12], while a previous study examined steel in an acidic medium without considering API-grade oil-well steel[13]. In contrast, the present work focuses on API P110 steel, a high-strength steel widely used in deep oil and gas wells because of its superior mechanical properties. Therefore, evaluating the inhibition performance of FCL extract on API P110 steel is of greater practical relevance for oil field applications.

FCL extract exhibited high inhibition performance, achieving inhibition efficiencies of 93.12%, 92.19%, and 92.08% according to potentiodynamic polarization, electrochemical impedance spectroscopy, and weight-loss measurements, respectively. These values are comparable to those previously reported for FCL extract on other steel substrates, with maximum inhibition efficiencies of approximately 90.0%[10], 95.7%[11], 92.5%[12], and 91.8%[13], confirming the excellent

Table 4 — Corrosion rate (*CR*)values for API P110 steel in 0.5M H_2SO_4 solution before and after addition of FCL (5000 ppm) extract at different temperatures and the corresponding inhibition efficiencies

	Blank	FCL	
T(*K*)	*CR*(*mg/h.cm*^{2})	*CR*(*mg/h.cm*^{2})	*IE* (%)
298	5.556± 0.0015	0.44± 0.0021	92.08
303	10.73± 0.0017	0.48± 0.0014	95.52
308	15.71± 0.0012	0.503± 0.0014	96.79
313	24.02± 0.0018	0.55± 0.0011	97.71

adsorption capability of the extract on different steel substrates and demonstrating the remarkable protection even for the more mechanically resistant API P110 steel.

Effect of temperature

The effect of temperature on the corrosion behaviour of API P110 steel in 0.5 M H_2SO_4 containing 5000 ppm of FCL extract was investigated using the weight-loss method.

Table 4 summarizes the corrosion rate and inhibition efficiency values obtained at different temperatures (298–313 K) in 0.5 M H_2SO_4. The results indicate that the inhibition efficiency increased with increasing temperature. The corrosion rate (CR) of API P110 steel increased with temperature in both the uninhibited and inhibited solutions. However, the corrosion rate remained significantly lower in the presence of the FCL extract than in the uninhibited solution over the entire temperature range investigated.

The results obtained in the present study compares favourably with those reported for other green inhibitors applied to API steels in acidic media. A previous study reported that *Aloe vera* leaves extract achieved inhibition efficiencies of 83.75% and 88.60%, as determined by potentiodynamic polarization (PDP) and electrochemical impedance spectroscopy (EIS), respectively, at an optimum concentration of 300 mg L^{-1} and 310 K[24]. Similarly, another study found that *Mitragyna speciosa* leaves extract exhibited a maximum inhibition efficiency of 90.24% for API 5L X65 steel under optimum conditions[25]. Another investigation reported that *Cuminum cyminum* extract reached a maximum inhibition efficiency of 91.83% at 400 ppm and 298 K; however, the inhibition efficiency decreased markedly with increasing temperature, falling to 78.63% at 318 K, indicating partial desorption of the inhibitor molecules from the steel surface[26]. In contrast, the present findings demonstrate that the inhibition efficiency of FCL extract increased with increasing temperature, reaching a maximum value of 97.71%, which suggests that

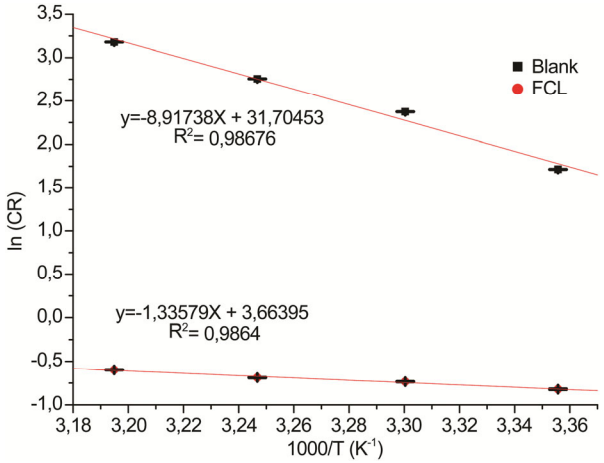

Fig. 4 — Arrhenius plots for the corrosion of API P110 steel in 0.5 M H_2SO_4 solution in the absence and presence of 5000 ppm FCL extract

adsorption becomes more favourable at elevated temperatures. Furthermore, inhibition efficiencies of 93.12%, 92.19%, and 92.08% were obtained at 298 K by potentiodynamic polarization, electrochemical impedance spectroscopy, and weight-loss measurements, respectively. These values are in excellent agreement with those reported for other plant-derived inhibitors, confirming the high protective performance of FCL extract against the corrosion of API P110 steel.

At a given temperature, a dynamic equilibrium exists between the adsorption and desorption of inhibitor molecules at the metal/solution interface[16]. As the temperature increases, this equilibrium shifts toward adsorption, resulting in greater surface coverage until a new equilibrium state is established[28]. Consequently, the inhibition efficiency increases with temperature, indicating the formation of a more stable protective film on the API P110 steel surface. This behaviour suggests that the adsorption of FCL extract is predominantly chemical in nature (chemisorption), although this assumption should be further supported by the thermodynamic parameters discussed in the following section.

The dependence of the corrosion rate on temperature can be described by the Arrhenius equation[15]:

$$CR = A \exp\left(-\frac{E_a}{RT}\right) \quad \ldots (7)$$

Where, "A" stands for the Arrhenius constant and "E_a" for the activation energy of corrosion. The activation energy (E_a) values were determined from the slopes of the Arrhenius plots presented in Fig. 4 and are

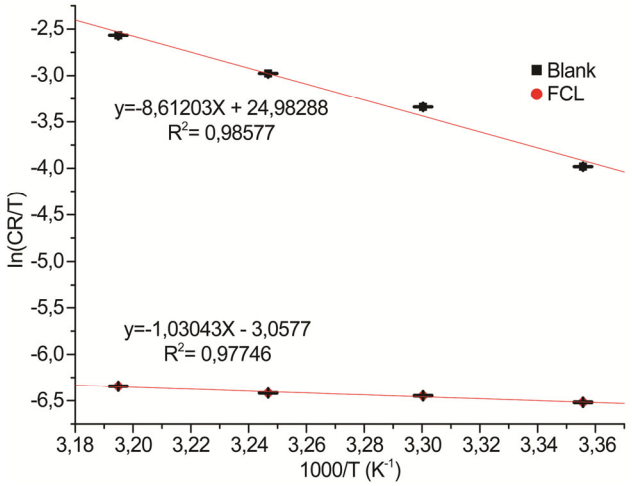

Fig. 5 — Transition-state plots for the corrosion of API P110 steel in 0.5 M H_2SO_4 solution in the absence and presence of 5000 ppm FCL extract

Table 5 — Activation energy values for the corrosion of API P110 steel in 0.5M H_2SO_4 solution without and with FCL extract

Extract	Blank	FCL
E_a (*KJ/mol*)	74.14	11.11

Table 6 — Activation enthalpy ($\Delta H°_a$) and activation entropy ($\Delta S°_a$) values for the corrosion of API P110 steel in 0.5 M H_2SO_4 solution without and with FCL extract

Extract	$\Delta H°_a$ (*KJ/mol*)	$\Delta S°_a$ (*J/mol.K*)
Blank	71.60	10.17
FCL	8.57	- 222.96

summarized in Table 5. The apparent activation energy in the inhibited solution was lower than that in the uninhibited solution. According to Radovici's classification[27], this behaviour corresponds to Class B inhibitors, for which the activation energy in the presence of the inhibitor is lower than that in the blank solution. This finding suggests that the adsorption of FCL extract on the API P110 steel surface is predominantly governed by chemisorption.

The activation enthalpy ($\Delta H°_a$) and activation entropy ($\Delta S°_a$) were determined using the transition-state equation[15]:

$$\ln\left(\frac{CR}{T}\right) = \ln\left(\frac{R}{N_a.h}\right) + \frac{\Delta S°a}{R} - \frac{\Delta H°a}{RT} \quad \ldots (8)$$

Where "N_a" stands for Avogadro's number and "h" for Planck's constant. The values of enthalpy ($\Delta H°_a$) based on plot slope and ($\Delta S°_a$) based on intercepts obtained from Fig. 5 are listed in Table 6. The positive value of $\Delta H°_a$ indicates that the dissolution of API P110 steel is an endothermic process[28].

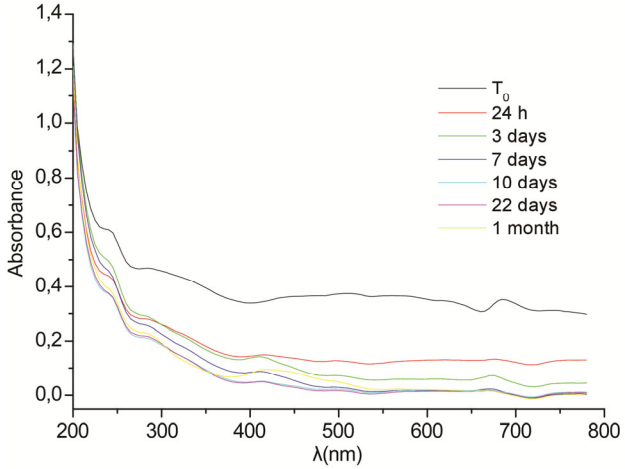

Fig. 6 — UV–visible spectra of FCL extract in 0.5 M H_2SO_4 solution: freshly prepared and after different storage periods up to one month

Furthermore, the positive value of $\Delta S°_a$ for the blank solution indicates an increase in disorder during the formation of the activated complex, suggesting a dissociation process in the rate-determining step[29]. In contrast, the large negative $\Delta S°_a$ value obtained in the presence of the FCL extract indicates that the activated complex is more ordered than the reactants, reflecting an association process during the rate-determining step[28]. This pronounced decrease in entropy may be attributed to the formation of a highly organized and stable adsorbed layer of FCL on the API P110 steel surface, thereby enhancing its corrosion protection.

Effect of time on solution storage

This part of the study aimed to evaluate the stability of the inhibitor solution over time by comparing the performance of freshly prepared solutions with that of solutions stored for different periods. UV–visible spectroscopy was employed to monitor the changes occurring in the inhibitor solution during storage. The UV–visible spectra of a solution containing 50 ppm FCL extract in 0.5 M H_2SO_4 were recorded over a storage period of one month at different time intervals, as shown in Fig. 6. The UV–visible spectra exhibit a similar profile throughout the storage period. The absorbance decreased during the first 24 h of storage and then remained nearly constant for up to one month. Moreover, the characteristic absorption bands in the 200–400 nm region remained clearly visible throughout the storage period, indicating that the main chemical constituents of the FCL extract

Table 7 — Corrosion rate (*CR*) and inhibition efficiency (*IE%)* of 5000 ppm FCL extract in 0.5 M H_2SO_4 solution measured immediately after preparation and after different storage periods up to one month for API P110 steel at 298 K.

Time	$CR(mg/h.cm^2) \times 10^{-4}$	*IE*(%)
/	5.11	93.88
24 h	6.48	92.26
3 days	7.41	91.12
7 days	7.25	91.30
10 days	7.00	91.60
22 days	6.48	92.26
1 month	4.23	92.38

were preserved and no significant degradation occurred.

Table 7 shows that the inhibition efficiency of the 5000 ppm leaves extract remained nearly constant throughout the storage period. This finding indicates that freshly prepared inhibitor solutions are not required for the effective corrosion protection of API P110 steel in 0.5 M H_2SO_4. The inhibitor solution retained its protective performance for up to one month of storage.

Adsorption isotherm

Adsorption isotherms can be used to understand the corrosion inhibition processes. According to Fig. 7, the inhibitor obeys Temkin adsorption isotherm given by the following formula[16]:

$$\theta = -\frac{\ln K}{2\alpha} - \frac{\ln C}{2\alpha} \quad \ldots (9)$$

Where "*K*" is the adsorption equilibrium constant and "α" is the Temkin interaction parameter, which reflects the interactions between adsorbed species. The Temkin isotherm considers the interactions between molecules adsorbed on the metallic surface[16]. The adsorption equilibrium constant K and the standard free energy ΔG^0_{ads} are related with the equation that follows[18]:

$$K = \frac{1}{10^6} \exp\left(\frac{-\Delta G^0_{ads}}{RT}\right) \quad \ldots (10)$$

Where, 10^6: concentration of water in solution (ppm), *R*: universal gas constant (8.314 J/mol K) and *T*: the absolute temperature.

Table 8 displays "*K*" and "ΔG^0_{ads}"values for steel adsorption. The negative value of ΔG^0_{ads} indicates that the adsorption of FCL extract molecules on the API P110 steel surface is a spontaneous process, leading to the formation of a stable protective layer. In general, ΔG^0_{ads} values around or less negative than −20 kJ mol^{-1} are associated with physical adsorption (physisorption), whereas values around or more

Table 8 — Thermodynamic parameters values for adsorption of FCL extract on API P110 steel surface in H_2SO_4 solution (0.5M) at 298K

Plant extract	$K\ (ppm^{-1})$	$\Delta G^0_{ads}\ (KJ/mol)$
FCL	1.68×10^{-2}	- 24.11

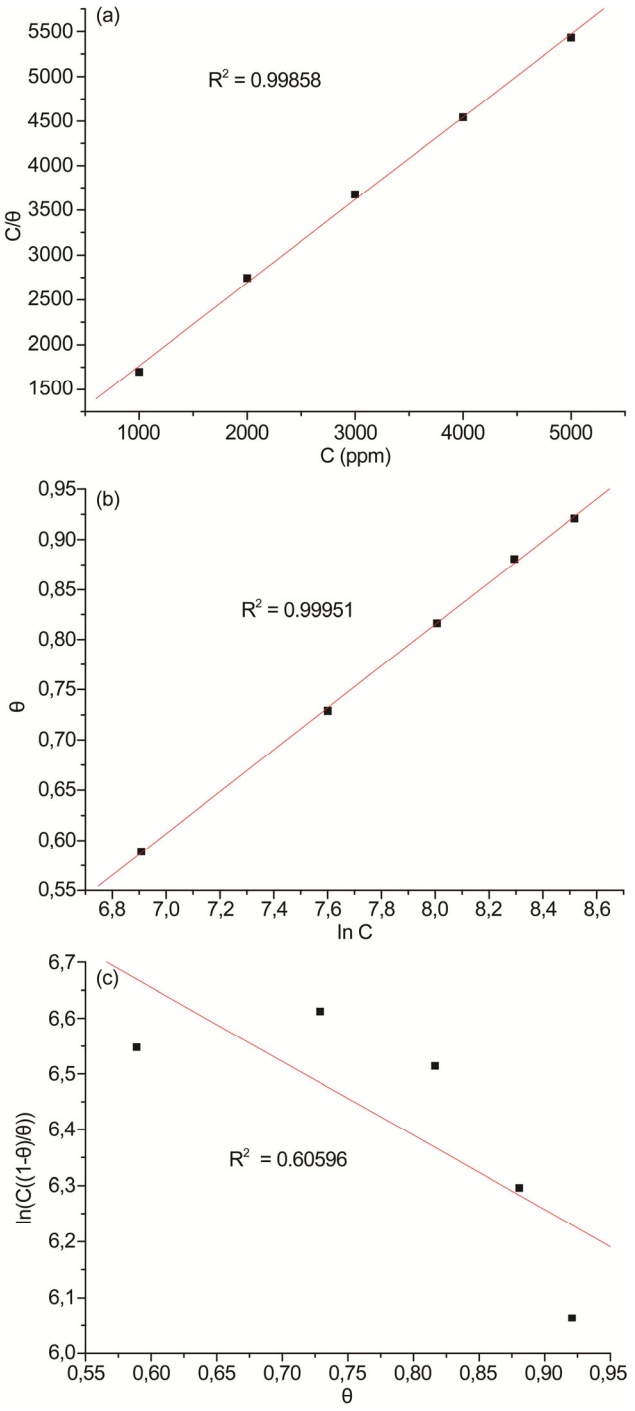

Fig. 7 — (a) Langmuir, (b) Temkin, and (c) Frumkin adsorption plots for FCL extract on API P110 steel in 0.5 M H_2SO_4 solution at 298 K

Table 9 — Inhibition efficiency (*IE*%) and synergism parameter (S) values at different concentrations of FCL extract without and with various concentrations of KI and KBr for API P110 steel in 0.5 M H_2SO_4 solution.

	IE (%)	*IE* (%) KBr (10^{-4} M)	S	*IE* (%) KBr (5×10^{-4} M)	S	*IE* (%) KI (5×10^{-6} M)	S	*IE* (%) KI (10^{-5} M)	S
Blank + KBr /+ KI	-	20.81	-	27.60	-	3.05	-	9.53	-
1000 ppm /+ KBr /+ KI	58.90	65.44	0.94	69.82	0.99	74.62	1.57	82.84	2.16
2000 ppm/ + KBr /+ KI	77.44	87.28	1.40	93.34	2.45	84.82	1.44	91.78	2.48
3000 ppm/ + KBr /+ KI	81.64	96.28	3.90	95.96	3.29	90.40	1.85	92.14	2.11
4000 ppm / + KBr /+ KI	85.24	95.78	2.76	97.19	3.80	93.40	2.16	93.94	2.20
5000 ppm / + KBr /+ KI	92.08	95.35	1.34	95.78	1.35	92.38	1	93.82	1.16

negative than −40 kJ mol^{-1} indicate chemical adsorption (chemisorption)[30]. The ΔG^0_{ads} value obtained in the present study lies between −20 and −40 kJ mol^{-1}, suggesting that the adsorption of FCL extract on the API P110 steel surface involves both physical and chemical interactions.

Effect of synergy

In corrosive media, the synergistic effect is a helpful technique for enhancing the performance of corrosion inhibitors while reducing the amount of inhibitor required. Synergism occurs when the combined action of two species provides greater inhibition efficiency than their individual effects. In particular, the addition of halide ions to an inhibitor solution can significantly improve the adsorption of inhibitor molecules on the metal surface. As a result, the inhibition efficiency of the combined inhibitor–halide system is higher than that achieved by either component used individually.

Aramaki *et al*. proposed two adsorption mechanisms to describe the synergistic effect observed when two inhibitors are present simultaneously in the corrosive medium. The synergistic effect can be quantitatively evaluated using the synergism parameter (S), which is calculated according to the following equation[31,32]:

$$S = \frac{[(1-\theta_1)(1-\theta_2)]}{(1-\theta_{1+2})} \quad \text{.... (11)}$$

θ_1: is the surface coverage measured in the presence of various concentrations of the extract.

θ_2: is the surface coverage determined in the presence of KI or KBr.

$\theta_{(1+2)}$: is the surface coverage ascertained in the presence of various concentrations of the extract with addition of KI or KBr.

The value of the synergism parameter (S) can be interpreted as follows [31,32]:

- S < 1 Competitive adsorption, the two species are adsorbed independently on different active sites of the metal surface.
- S > 1 Cooperative adsorption, one species is chemisorbed onto the metal surface, while the other is subsequently physisorbed onto the chemisorbed layer.

Table 9 reorganizes the study findings about the synergistic effect on steel corrosion. An improvement in inhibition efficiency values for various extract concentrations is demonstrated by the data in Table 9. Values are better improved with KI than KBr at lower concentrations (5×10^{-6} M). Further tests showed that increasing the concentration of KBr to 10^{-3} M and KI to 10^{-4} M enhanced inhibitory efficiencies, reaching values greater than 99% for all concentrations of the extract.

The observed enhancement in inhibition efficiency can be attributed to the synergistic interaction between the halide ions and the FCL extract. According to previous studies, the synergistic effect of halide ions combined with organic inhibitors in acidic media follows the order I^-> Br^-> Cl^-. Iodide ions generally exhibit the strongest synergistic effect because of their larger ionic radius, lower oxidation potential and higher electronic polarizability, which facilitate electron transfer and stabilize intermediate species more effectively. These properties enhance its ability to act as a redox mediator, thereby accelerating the overall process compared to bromide[33]. Consequently, KI produced a stronger synergistic effect than KBr, in agreement with the trend reported in the literature.

According to Aramaki's criterion, the "S" values obtained are greater than unity, indicating that cooperative adsorption occurs between the *Ficus carica* leaves extract molecules and Br^- or I^- ions on the API P110 steel surface.

The synergistic inhibition observed in the presence of FCL extract and halide ions can be explained by

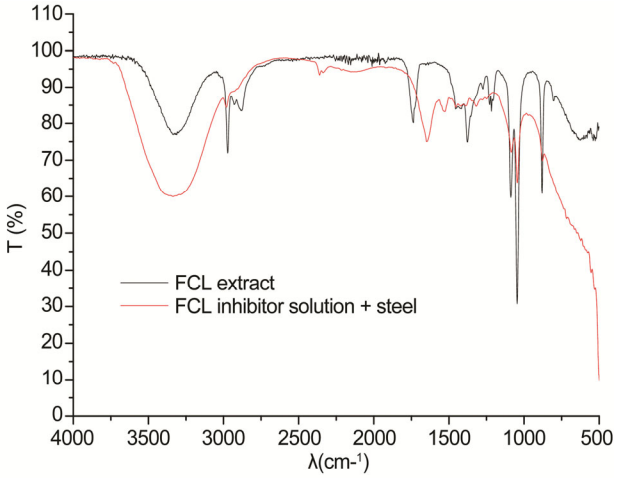

Fig. 8 — FTIR spectra of FCL extract and API P110 steel after immersion in the inhibitor solution

the interaction between the protonated phytochemical constituents of the extract and the strongly chemisorbed Br^- or I^- ions on the API P110 steel surface. The halide ions are first chemisorbed onto the positively charged metal surface, creating adsorption sites that facilitate the subsequent physisorption of the protonated inhibitor molecules through electrostatic (Coulombic) attraction. This cooperative adsorption results in the formation of a more compact and stable protective film, thereby significantly enhances the corrosion inhibition efficiency[34].

Although a previous study demonstrated the synergistic effect of KI with *Capsicum annuum* extract for API P110 steel in 15 wt.% HCl, their study was limited to iodide ions[14]. The *Capsicum annuum* extract alone achieved a maximum inhibition efficiency of 89.5%, which increased to 92.2% after the addition of KI, confirming the beneficial effect of iodide ions on corrosion inhibition. In contrast, the present study provides a systematic comparison of the synergistic effects of both iodide and bromide ions combined with FCL extract for API P110 steel in 0.5 M H_2SO_4. Moreover, the optimum concentrations of KI and KBr were determined, resulting in inhibition efficiencies exceeding 99%. These findings demonstrate not only the superior inhibition performance of the *Ficus carica*/halide systems but also provide new insights into the comparative role of iodide and bromide ions in enhancing the adsorption and corrosion protection of API P110 steel.

FTIR spectra

Fig. 8 presents the FTIR spectra of the FCL extract and the API P110 steel after immersion in the inhibitor solution, allowing the identification of the functional groups involved in the adsorption process. The FTIR spectrum of *Ficus carica* leaves extract exhibits a broad absorption band around 3400 cm^{-1}, which is attributed to the stretching vibrations of hydroxyl (O–H) groups. The bands observed between 2800 and 3000 cm^{-1} are assigned to the symmetric and asymmetric stretching vibrations of C–H bonds. The absorption band at approximately 1750 cm^{-1} corresponds to the stretching vibrations of the carbonyl (C=O) groups. The weak band around 1200 cm^{-1} is attributed to the C–O–C stretching vibrations, while the intense bands in the 1150–1000 cm^{-1} region are assigned to C–O stretching vibrations[35].

The broad absorption band around 3400 cm^{-1} (attributed to hydroxyl (O–H) groups), the intense bands in the 1150–1000 cm^{-1} region (assigned to C–O stretching vibrations), and the carbonyl (C=O) absorption band shifted from approximately 1750 cm^{-1} in the FCL extract spectrum to around 1650 cm^{-1} in the spectrum of the steel surface after inhibition are all observed in both spectra. This confirms the adsorption of FCL extract molecules through carbonyl and hydroxyl groups on the API P110 steel surface.

Scanning Electron Microscopy (SEM)

Scanning electron microscopy (SEM) was employed to examine the surface morphology of API P110 steel before and after immersion for 2 h in 0.5 M H_2SO_4 solution without and with FCL extract, FCL + KBr, and FCL + KI. The corresponding SEM micrographs are regrouped in Fig. 9. Fig. 9(a) shows that the API P110 steel surface is relatively smooth, with only a few fine scratches resulting from the polishing process. Fig. 9(b) reveals a severely damaged surface after immersion in 0.5 M H_2SO_4, characterized by numerous microcracks and microcavities caused by the aggressive attack of the acidic medium. In contrast, Fig. 9(c) shows that the presence of FCL extract significantly reduced the surface damages, resulting in a smoother surface than that observed in Fig. 9(b). Furthermore, Fig. 9(d) demonstrates that the addition of KBr provided additional protection, while the most pronounced improvement was observed for the FCL + KI system (Fig. 9(e)), where the steel surface remained nearly intact, with only the polishing marks still visible.

These SEM observations are in good accordance with the FTIR results, which confirmed the adsorption of FCL extract molecules on the steel surface through

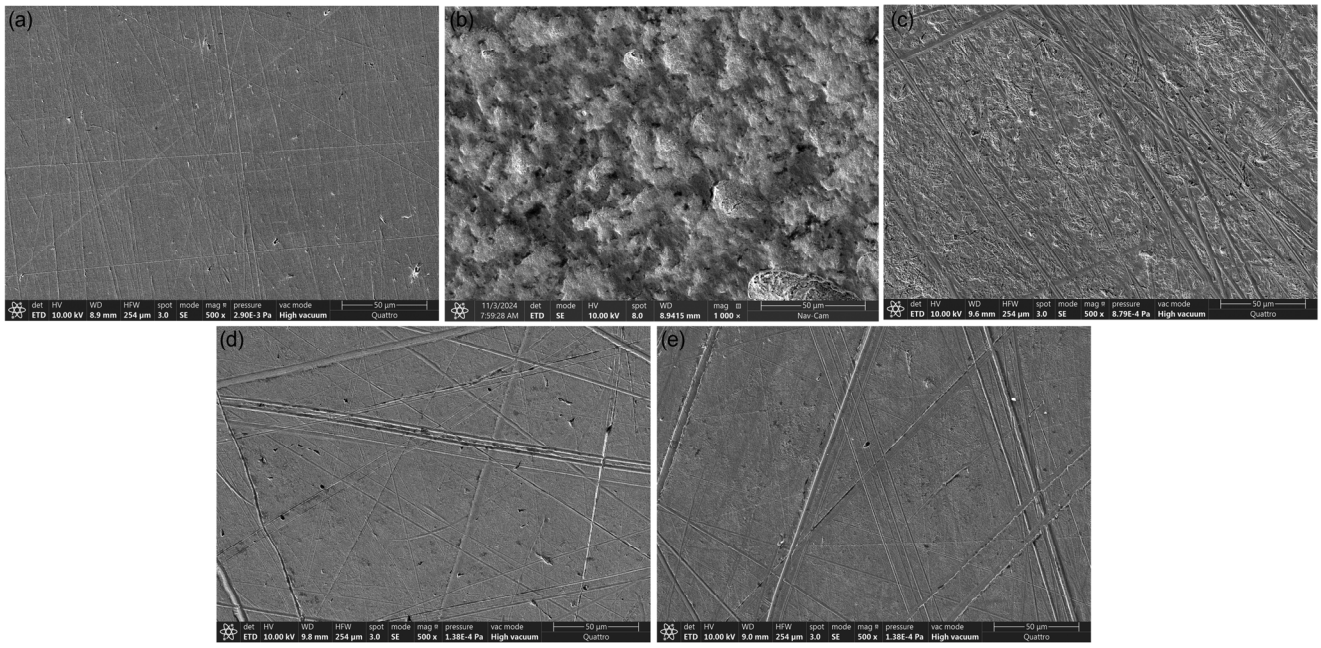

Fig. 9 — SEM images of (a) API P110 steel, (b) API P110 steel after immersion in 0.5 M H_2SO_4, (c) API P110 steel after addition of FCL extract (5000 ppm), (d) API P110 steel after addition of FCL extract (5000 ppm) and 10^{-2}M KBr, and (e) API P110 steel after addition of FCL extract (5000 ppm) and 10^{-2} M KI

hydroxyl and carbonyl functional groups. The adsorption of these phytochemical constituents leads to the formation of a compact and stable protective film that effectively isolates the metal surface from the aggressive acidic medium. The improved surface morphology observed in the presence of both KBr and KI further supports the synergistic interaction between the halide ions and the adsorbed FCL extract molecules, resulting in enhanced corrosion protection. The more uniform and less damaged surface obtained with KI indicates that iodide ions provide a stronger synergistic effect than bromide ions.

Limitations and future perspectives

Although the present study demonstrates the effective corrosion inhibition performance of FCL extract for API P110 steel in 0.5 M H_2SO_4 under laboratory conditions, some limitations should be acknowledged. The experiments were carried out in a static acidic medium at controlled temperature, whereas oil-field acidizing operations involve more complex conditions, including high pressure, elevated temperatures, turbulent flow, and the presence of dissolved gases (CO_2 and H_2S), salts, and other chemical additives. Therefore, the inhibitor performance under actual field conditions remains to be evaluated. Future work should focus on validating the effectiveness of the FCL extract–halide system under simulated and real oil-field environments, investigating its long-term stability, compatibility with commercial acidizing fluids, and environmental impact before large-scale industrial application.

Conclusion

The present study demonstrates that *Ficus carica* leaves extract is an effective and environmentally friendly corrosion inhibitor for API P110 steel in 0.5 M H_2SO_4 solution. The inhibitor exhibited good corrosion protection, and its performance was further enhanced by the synergistic action of iodide and bromide ions, resulting in improved adsorption and the formation of a stable protective film on the steel surface. Unlike several recently reported green inhibitors for API steels, the inhibition efficiency of *Ficus carica* leaves extract increased with temperature, reaching a maximum value of 97%, highlighting its excellent thermal stability and suitability for high-temperature acidic environments. These findings indicate that *Ficus carica* leaves extract represents a promising sustainable alternative to conventional synthetic corrosion inhibitors for oilfield acidizing operations. Moreover, this work extends the application of plant-based inhibitors to high-strength API P110 steel, for which only limited information is currently available, and provides useful insights for the development of eco-friendly corrosion protection strategies in the petroleum industry.

Conflict of Interest

The authors declare that there are no conflicts of interest associated with this work.

References

1 Jasim Z I, Rashid K H & Khadom A A, Corrosion and corrosion control of the steel in acidizing oil wells: Processes-An overview of organic inhibitors, *Russ J Appl Chem*, 97 (2024)

2 Díaz-Jiménez V, Gómez-Sánchez G, Likhanova N V, Arellanes-Lozada P, Olivares-Xometl O, Lijanova I V & Arriola-Morales J, Current overview of corrosion inhibition of API steel in different environments, *ACS Omega*, 9 (2024) 27798**.**

3 Solomon M M, Uzoma I E, Olugbuyiro J A O & Ademosun O T, A censorious appraisal of the oil well acidizing corrosion inhibitors, *J Pet Sci Eng*, 215 (2022) 110711.

4 Wasim M & Djukic M B, External corrosion of oil and gas pipelines: A review of failure mechanisms and predictive preventions, *J Nat Gas Sci Eng*, 100 (2022) 104467.

5 Wan H, Li C, Wang Z, Liu R & Chen C, Corrosion behavior of P110S oil casing steel in sulfur containing environment, *J Chin Soc Corros Prot*, 43 (2023) 371.

6 Minagalavar R L, Rajappa S K, Rathod M R & Sajjan A M, Investigation of *Laurus tamala* leaves extract as an environmentally acceptable corrosion inhibitor for soft steel in 1 M HCl: Electrochemical, DFT and surface characterization techniques, *Indian J Chem Technol*, 30 (2023) 492.

7 Macadangdang R R , Corrosion inhibition, adsorption behaviour, and thermodynamic studies of red dragon fruit (*Selenicereus costaricensis*) waste peel extracts on mild steel in acidic environment, *Indian J Chem Technol*, 29 (2022) 201.

8 Nomozov A K, Beknazarov K S, Khodjamkulov S Z & Misirov Z K, *Salsola oppositifolia* acid extract as a green corrosion inhibitor for carbon steel, *Indian J Chem Technol*, 30 (2023) 872.

9 Sinha R R, Rajak D K, Gope L, Singh S K & Mishra S P, Study of N-(3-chloro-2-phenyl)-4-oxozetiden-1-yl)-isonicotinamide as a corrosion inhibitor of mild steel in acidic environment, *Indian J Chem Technol*, 31 (2024) 451.

10 Ibrahim T H, Gomes E E, Obot I B, Khamis M & Sabri M A, Mild steel green inhibition by *Ficus carica* leaves extract under practical field conditions, *J Adhes Sci Technol*, 31 (2017) 2473.

11 El-Zekred M A, Nofal A M, Shalabi K & Fouda A S, *Ficus carica* extract as environmentally friendly inhibitor for the corrosion of L-80 carbon steel in 0.5 M H_2SO_4 media, *J Indian Chem Soc*, 98 (2021) 100128.

12 Ghalib L, Abdulghani H A & Hamad A J, A comparative study on inhibitory action of *Ficus carica*, *Olea europaea* and *Ziziphus spina-christi* plant leaves on carbon steel in sulfuric acid medium, *AIP Conf Proc*, 2213 (2020) 020180.

13 Rahmouni H, Nigri S & Nacef M, Analysis of Fig leaf extract as steel eco-friendly corrosion inhibitor in acidic medium, *Anal Bioanal Electrochem*, 16 (2024) 142.

14 Singh A, Ansari K R, Ali I H, El Ibrahimi B, Alanazi A K, Younas M, Singh T & Lin Y, Synergistic mixture of *Capsicum annuum* fruit extract/KI as an efficient inhibitor for the corrosion of P110 steel in 15% HCl solution under hydrodynamic condition, *Z Phys Chem*, 238 (2024) 339.

15 Deyab M A & Mohsen Q, An eco-friendly corrosion inhibitor for steel used in desalination systems during acid cleaning: Irish ivy extract, *Sci Rep*, 14 (2024) 30505.

16 Yang X, Zhou Y, Wang L, Li Z, Wang J & Zhang Y, Chestnut shell aqueous extract as a green efficient corrosion inhibitor for acid-cleaning carbon steel, *Sci Rep*, 15 (2025) 8798.

17 Ferreira E S, Giacomelli C, Giacomelli F C & Spinelli A, Evaluation of the inhibitor effect of L-ascorbic acid on the corrosion of mild steel, *Mater Chem Phys*, 83 (2004) 129.

18 Abdelaziz M, El-Ibrahimi B, El Mouaden K, Bazzi L & Hilali M, Orange peel extract as an eco-friendly corrosion inhibitor for carbon steel in hydrochloric acid solution, *Sci Rep*, 13 (2023) 21943.

19 Elabbasy H M, Elnagar M E & Fouda A S, Chemical, electrochemical and surface studies of *Rosa damascena* extract as a green corrosion inhibitor for carbon steel in sulfuric acid environment, *J Chin Chem Soc*, 71 (2024) 385.

20 Hamood A F, Habeeb H M, Abdulhussein B A, Mustafa A M, Sayyid F F, Hanoon M M, Gaaz T S, Hameed L A & Alamiery A A A, Weight loss, electrochemical measurements and DFT studies on corrosion inhibition by 7-mercapto-4-methylcoumarin, *Results Eng*, 23 (2024) 102677.

21 Boulkroune M, Dekkiche B & Abassi Y, *Peganum harmala* seeds as a sustainable source of pickling inhibitor for zinc, *Anal Bioanal Electrochem*, 15 (2023) 394.

22 Barsoukov E & Macdonald J R, *Impedance* Spectroscopy: Theory, Experiment, and Applications, 3rd Edn (John Wiley & Sons, Hoboken), (2018).

23 Wu J, Tang M, Deng S & Li X, Adsorption behavior and inhibition performance of 2-amino-5-bromothiazole on steel surface in HCl solution, *Results Eng*, 30 (2026) 110723.

24 Royani A, Hanafi M, Mubarak N M, Priyotomo G, Aigbodion V S, Musabikha S & Manaf A, Unveiling green corrosion inhibitor of *Aloe vera* extracts for API 5L steel in seawater environment, *Sci Rep*, 14 (2024) 14085.

25 Okuma S O, Nwaeju-Okechukwu C C & Oreko B U, Adsorption, kinetic, thermodynamic, thermal stability, and RSM optimization studies of *Mitragyna speciosa* as a green corrosion inhibitor for API 5L X65 steel in aggressive oil and gas well treatment fluids, *Chem Thermodyn Therm Anal*, 22 (2026) 100287.

26 Fouda A S, Rashwan S, Ibrahim H, Reda M, Eissa M E & El-Hossiany A, *Cuminum cyminum* as green corrosion inhibitor for API 5L X70 carbon steel in 0.5 M H_2SO_4 solution, *Sci Rep*, 15 (2025) 17120.

27 Radovici O, Heterogeneous catalysis: Principles and applications, Proceedings of the 7th European Symposium on Corrosion Inhibitors (Ferrara, Italy), (1990) 330.

28 Ibeji C U, Akintayo D C, Oluwasola H O, Akintemi E O, Onwukwe O G & Eziomume O M, Synthesis, experimental and computational studies on the anti-corrosion performance of substituted Schiff bases of 2-methoxybenzaldehyde for mild steel in HCl medium, *Sci Rep*, 13 (2023) 3265**.**

29 Abo-El-Ela F I, El-Mahdy G A, El-Mallah A M & El-Mahdy A M, Corrosion inhibition of carbon steel using citrus peel extract in acidic medium: Experimental and theoretical studies, *Int J Corros Scale Inhib*, 13 (2024) 1687**.**

30 Sahraoui M, Boulkroune M & Chibani A, Aqueous extract of *Punica granatum* fruit peel as an eco-friendly corrosion inhibitor for aluminium alloy, *J Bio Tribo Corros*, 8 (2022) 54.
31 Aramaki K, Hagiwara M & Nishihara H, The synergistic effect of anions and the ammonium cation on the inhibition of iron corrosion in acid solution, *Corros Sci*, 27 (1987) 487.
32 Hosny S, Abdelfatah A & Gaber G A, Synthesis, characterization, synergistic inhibition, and biological evaluation of novel Schiff base on 304 stainless steel in acid solution, *Sci Rep*, 14 (2024) 470.
33 Ahmed M A, Amin S & Mohamed A A, Current and emerging trends of inorganic, organic and eco-friendly corrosion inhibitors, *RSC Adv*, 14 (2024) 31877.
34 Messikh S & Salhi R, *Etude de l'inhibition de la corrosion d'acier doux par des composés organiques en milieu acide*, (2024) 1.
35 Rashid A, Khan A & Dar S, Phytochemical profiling and FTIR spectroscopic characterization of *Ficus carica* leaves extract, *South Afr J Bot*, 146 (2022) 675.